Long-range proton transfer in aqueous acid-base reactions

B. J. Siwick*, M. J. Cox, and H. J. Bakker

FOM Institute AMOLF, Kruislaan 407, 1098 SJ Amsterdam, The Netherlands

(October 2, 2007)

Abstract

We study the mechanism of proton transfer (PT) in the aqueous acid-base reaction between the photo-acid 8-hydroxy-1,3,6-pyrenetrisulfonic acid (HPTS) and acetate by probing the vibrational resonances of HPTS, acetate and the hydrated proton with femtosecond mid-infrared laser pulses. We find that PT takes place in a distribution of hydrogen-bound reaction complexes that differ in the number of water molecules separating the acid and the base. The number of intervening water molecules ranges from 0 to 5, which together with a strongly distance-dependent PT rate explains the observed highly non-exponential reaction kinetics. The kinetic isotope effect for the reaction is determined to be 1.5, indicating that tunnelling does not play a significant role in the transfer of the proton. Rather, the transfer mechanism is best described in terms of the adiabatic proton transfer picture as it has been formulated by J. T. Hynes and coworkers [1,2], where solvent fluctuations play an essential role in forming the correct hydrogen-bond configuration and solvent polarization to facilitate PT.

* Present address: Departments of Physics and Chemistry, McGill University, Montreal, Canada

INTRODUCTION

Proton-transfer (PT) reactions are essential chemical processes that are ubiquitous in nature. The overall reaction equation for PT between an acid and a base looks deceptively simple: $AH + B^- \rightarrow A^- + BH$. However, the reaction can in fact be extremely complicated due to the involvement of the solvent molecules not shown in this equation. This is especially true in protic solvents like liquid water [3,4], which form hydrogen-bonded networks in which protons are highly mobile.

In their pioneering work on bimolecular PT in solution, Eigen and Weller distinguished three possible roles for water in enabling the reaction between a dissolved acid and a base. In the first role, water provides the passive medium in which the acid and the base diffuse to form a sterically favorable (hydrogen-bonded) encounter complex inside which PT can proceed. Inside the encounter complex water can have one of two possible additional roles as direct participant in the PT reaction by I) temporarily taking up a proton from the acid or II) releasing a proton to the base, thereby forming hydrated protons or hydroxide ions. The PT reaction is completed when either the hydrated proton (case I) migrates from the acid to the base, or the hydroxide ion (case II) migrates from the base to the acid. This two-stage picture involving 1) diffusive formation of a reactive encounter complex followed by 2) PT at some intrinsic rate has been denoted the Eigen-Weller framework for intermolecular acid-base reactions [3–6]. The quantitative implementation of this framework has typically been based on Smoluchowskis theory of diffusion-controlled reactions [7] extended to include a finite reaction rate on contact [8,9]. This description is denoted the Smoluchowski-Collins-Kimball (SCK) model, and is based on the spherically symmetric diffusion equation; i.e. the acid and the base diffuse to a certain intermolecular separation at which the PT reaction takes place.

As implied by the discussion above, the reactive complex can involve either a single hydrogen bond or a hydrogen bonded bridge/wire of water molecules connecting the proton donating group of the acid with the proton accepting group of the base. In fact, Eigen

inferred that the optimal distance for proton transfer is ~0.75 nm, which would correspond to a configuration in which the acid and the base are separated by approximately two water molecules [3,4]. The transfer of the positively charged proton within the reaction complex leads to a large change in polarity. Hence, in a polar solvent like water, the proton transfer is accompanied by strong electronic and dipolar rearrangements. Thus, water has a further role in the PT reaction (or charge-transfer reactions in general): the stabilization/destabilization of the various charge transferred species. Solvent fluctuations and (electronic) reorganizations play an essential role in the mechanism and rate of the reaction.

Much modern theoretical work has been directed at understanding the role of the solvent in this regard. In the work of J. T. Hynes, which is being celebrated through this special issue, different regimes for proton transfer have been distinguished depending on the strength of the hydrogen bond connecting the acid and the base and the strength of the interactions with the solvent [1,2]. If the acid and the base form a weak hydrogen bond, the potential in the proton coordinate is a double-well with a significant barrier separating reactant and product species. Proton transfer between acid and base in this regime, therefore, requires tunneling. The solvent plays a role in this transfer because solvent fluctuations can tune the vibrations on both sides of the barrier into resonance, thereby strongly increasing the tunnelling probability. This regime is called the non-adiabatic PT regime. If both the hydrogen bond between the acid and the base and the interactions with the solvent are strong, however, the proton can be transferred from the acid and the base by adiabatically following the solvent fluctuations without tunnelling. In this adiabatic PT regime, the reactant (proton at the acid) is first destabilized by solvent fluctuations which modulate the proton potential. As a result, the ground-state vibrational level of the proton becomes higher than the barrier and the proton becomes fully delocalized over the double well potential. Subsequent stabilization of the reactants by the solvent leads to a localization of the proton in the well at the base. It was found that this regime applies to the dissociation of HCl [2] and HF [10] in water.

The rate and mechanism of intermolecular proton transfer in aqueous media have been

extensively studied with experimental techniques, including time-resolved absorption and fluorescence spectroscopy [11–23]. Many of these studies employed the photo-acid pyranine: 8-hydroxy-1,3,6-pyrenetrisulfonic acid trisodiumsalt (HPTS). This photo-acid has a strong absorption near 400 nm and can thus easily be excited using the second harmonic of a Ti:sapphire laser. The excitation leads to an enhancement in the acidity of the molecule by a factor of 10^6. HPTS has been used to study the dynamics of acid dissociation [11–16] and acid-base reactions [17–23] using different time-resolved spectroscopic techniques. It was found that HPTS* dissociation in water (PT to solvent) occurs with a time constant of 90/220 ps in H_2O/D_2O. When a stronger base than water is added in sufficient concentration, the PT reaction speeds up significantly because intermolecular PT between the acid and the base (rather than PT to solvent) becomes the dominant reaction pathway. The direct PT between HPTS and acetate in H_2O/D_2O has been successfully modeled within the SCK framework using an intrinsic bimolecular reaction rate with a very strong isotope effect: $1.6{\times}10^{11}$ M^{-1} s^{-1} in H_2O and $4{\times}10^{10}$ M^{-1} s^{-1} in D_2O [18]. A suprising feature of these results is that the kinetic isotope effect (KIE) determined for direct PT between HPTS and acetate with a value of 4 is larger than the KIE determined for the PT to solvent. This is contrary to the expectation that the KIE should decrease as the reaction asymmetry increases [24].

Recently, the groups of Nibbering and Pines studied the intermolecular proton transfer between HPTS and different carboxylate bases by probing the vibrations of the photo-acid and an accepting base with femtosecond mid-infrared laser pulses [19–23]. In addition to a slow diffusive component that was successfully modeled with the SCK approach, they observed two other contributions to the signal: a fast component with a time constant of $\sim$ 150 fs that is due to proton transfer in direct contact pairs of the acid and the base, and a slower component with a time constant of 6 to several tens of picoseconds that was ascribed to PT in so-called loose reaction complexes. Both of these additional components were thought to have their origin in acid-base complexes that are present in the solution prior to the excitation of the HPTS molecule.

Here we investigate the role of the solvating water in facilitating intermolecular PT between HPTS and acetate in aqueous solution by probing the vibrational responses of HPTS, acetate and the broad-band infrared response of the hydrated proton/deuteron with femtosecond mid-infrared laser pulses. We find that PT occurs in a distribution of reaction complexes that differ in the number of water molecules separating the acid and base; Proton transfer in this system is long-range in character. We describe an extension of the classic Eigen-Weller framework based on this long-range PT that provides a more complete picture of these reactions, and discuss our findings in connection with the description of adiabatic proton transfer developed by J. T. Hynes [1,2].

EXPERIMENTAL

The proton transfer reaction between HPTS and acetate is studied with femtosecond visible pump-mid-infrared probe spectroscopy using a 1 kHz regeneratively amplified Ti:sapphire laser system (SpectraPhysics Hurricane). This system delivers 100 fs pulses centered at 800 nm with a total pulse energy of 1.0 mJ. The pump pulses used have a wavelength of 400 nm and are generated via second-harmonic generation of a fraction (0.2 mJ) of the laser output in a 1 mm thick BBO (β-bariumborate) crystal. The generated 400 nm pulses have an energy of 3 μJ and a pulse duration of 120 fs.

The mid-infrared probe pulses are generated via a sequence of nonlinear frequency-conversion processes. The first process of this sequence is white-light seeded optical parametric amplification in BBO (SpectraPhysics OPA). The white light generation and parametric amplification processes are pumped with 800 nm pulses with a total energy of 0.8 mJ, representing another fraction of the output of the Ti:sapphire regenerative amplifier. The parametric amplification results in two output pulses of which one is tunable between 1200 and 1600 nm (signal), and the other between 1600 and 2400 nm (idler). The signal and idler are used as input in a difference-frequency mixing process in $AgGaS_2$. In this process pulses with wavelengths tunable between 2.7 and 8 μm are generated, with a typical pulse

duration of ~150 fs, an energy of 1 μJ, and a frequency bandwidth of 200 cm^{-1}.

The samples studied are solutions of pyranine (8-hydroxy-1,3,6-pyrenetrisulfonic acid trisodiumsalt (HPTS, 98%) and the base NaCH$_3$COO in H$_2$O and D$_2$O. Both HPTS and NaCH$_3$COO were purchased from Aldrich and are used without further purification. In most experiments, the concentration of HPTS was 10 mM. The concentration of acetate base was 0, 0.5, 1, 2, and 4 M. Part of the HPTS (with a maximum of 50% at 4 M acetate) reacts with acetate to form the conjugate base (PTS^{*-}), thereby forming self-buffering solutions. We performed control experiments on solutions containing only the conjugate base, and found no signal following excitation at 400 nm, except during temporal overlap of the 400 nm excitation pulse and the mid-infrared probing pulses (i.e. <200 fs). We have also performed experiments on pH balanced solutions (obtained by adding small amounts of acetic acid), and the results were found to be identical to those without buffering. The 400 nm pump pulse is resonant with the red wing of a strong absorption band of HPTS that is centered at 365 nm [14]. The excitation of this band switches the pK$_a$ of the HPTS molecules from ~7 to a value of ~1 [25], an enormous enhancement in acidity. It is important to note, however, that despite the large increase in K$_a$, that HPTS* is still a weak acid (i.e. pK$_a^* >$0). The acid ionization reaction only goes to completion due to the dilute concentration of HPTS. The infrared probe pulse are tuned to resonances of the excited HPTS*, the conjugated photo base PTS^{*-}, the hydrated proton/deuteron, and the carbonyl vibration of acetic acid. As a result, all stages of the proton-transfer reaction are detected.

The sample is contained in a flow-cell with CaF$_2$ windows and an optical path length of 10-50 μm, depending on the solution. The pump pulses are focussed in the sample using a CaF$_2$ lens with a focal length of 20 cm to a focus with a diameter of 100 μm. The probe pulses are sent on a wedged CaF$_2$ plate. The front side reflection (~5 %) is focussed within the focal volume of the pump pulse using a parabolic mirror with a focal length of 10 cm. The probe light transmitted through the sample is dispersed with an Oriel monochromator and detected with one line of an Infrared Associates 2×32 MCT (mercury-cadmium-telluride) detector array. The reflection off the back side of the wedged CaF$_2$ plate is also focussed

in the sample, but not in overlap with the pump. This fraction is also dispersed by the monochromator and detected by the second line of the MCT detector array. This signal is used as a reference in the experiment to enable a frequency-resolved correction for shot-to-shot fluctuations in the probe-pulse energy. The probe polarization is rotated to the magic angle so that only isotropic absorption changes are detected and the measurements are not affected by molecular reorientations.

CONDUCTION MODEL FOR INTERMOLECULAR PROTON TRANSFER

Recently it was shown that the SCK model does not provide an adequate description of the reaction between HPTS and acetate at all delay times [19,20,26]. The SCK model provides either a good description of the data at short delay times by using a large on-contact reaction rate, or a good description of the data at large delay times using a lower on-contact reaction rate [26]. This discrepancy is likely due to a number of model assumptions that are not entirely appropriate for PT reactions in aqueous solution. A significant deficiency of the SCK approach is that spherical symmetry is assumed for the reactive encounter complex. Clearly, acidic molecules are in general not isotropically reactive, and important orientational constraints have to be satisfied before the reaction can proceed. Since reorientation of HPTS occurs on timescales much longer than either PT or translational diffusion over molecular length scales (the rotational diffusion time for HPTS in water is ∼150 ps [20]), spherical symmetry cannot be assumed even in the average sense. In addition, it has been shown that water provides an excellent medium to conduct protons via an exchange of chemical bonds and hydrogen bonds [27–29]. Therefore, it is far from evident that proton transfer should be taken to occur at a fixed reaction radius, as is assumed in the SCK model. A final problem is that the SCK model ignores the discrete nature of the solvent and the structure of the aqueous hydrogen bond network. Both of these features are expected to be important for intermolecular proton transfer, since bond making/breaking is an essential feature of these charge transfer reactions (unlike outer-shell electron transfer).

To account for the effects of the hydrogen-bond structure, its fluctuations, and the possibility of long-range PT through this network, we have developed a new model for PT. In the model we consider that proton transfer takes place in reaction complexes of the type:

$$RO *^- \cdots H^+ \cdots (OH_2)_{n-1} \cdots B^a, \tag{1}$$

where $RO *^- \cdots H^+$ denotes the acid, $(OH_2)_{n-1}$ the number $(n-1)$ of intervening water molecules, and a the number of base (B) accepting sites in the n'th solvation shell of the acid. In the case of acetate each oxygen atom forms a possible accepting site for the proton. The distribution of such complexes initially present in solution is assumed to be statistical, which implies that this distribution is dictated by the base concentration. With increasing base concentration, the relative fraction of complexes with a small number of intervening water molecules will increase. We assume that the hydrogen-bond network of the solvation shells is branched in such a way that the number of available oxygen positions doubles for every subsequent shell. Hence, shell n contains 2^{n-1} oxygen positions. The reasoning behind this structure is that every water molecule has two OH groups and can thus donate two hydrogen bonds over which the proton charge can be transferred. This is a good assumption for small shell numbers, but progressively worsens as n becomes large. This point is discussed below. The model is illustrated in Fig. 1a.

The relative probabilities of occurrence for the different reaction complexes or states is denoted $S[n, a]$, where n is the shell number containing the closest acetate oxygen atom, and a denotes the number of acetate oxygen atoms in that shell. Before the reaction starts $(t = 0)$ these probabilities are given by:

$$S[n, a](0) = P_w^{(2^{n-1}-1)} \binom{2^{n-1}}{a} P_a^a P_w^{(2^{n-1}-a)}, \tag{2}$$

where P_w represents the fraction of oxygen atoms in the solution belonging to water molecules and P_a represents the fraction of oxygen atoms belonging to acetate molecules. The first factor in equation (2) represents the probability that all oxygen atoms up to shell n are water oxygen atoms. The latter factor represents the probability that there are a acetate

oxygen atoms in shell n. The values of P_w and P_a are determined by the concentration of acetate: $P_a = 2[Ac]/(55 - 2[Ac])$ and $P_w = 1 - P_a$. The factor of 2 follows from the fact that every acetate contains two oxygen atoms. It can easily be shown that the distribution over the states is normalized: $\sum_n \sum_a S[n, a] = 1$. The assumption in the model that the number of oxygen atoms doubles with each additional solvation shell is an approximation of the real hydrogen-bond structure of the liquid. The increase in the number of oxygen atoms when going to the next higher shell will in reality be smaller than two for several reasons. In the first place, there is a non-zero probability that an OH group of a water molecule does not donate a hydrogen bond to the oxygen atom of a next water molecule. Second, the hydrogen bond may be donated to an oxygen atom of a water molecule that is located in an earlier shell. In that case the hydrogen-bonded water wire forms a closed loop that cannot conduct the proton to an oxygen atom of an accepting carboxylate base. This latter effect will become more important when the concentration of carboxylate base is low. At higher base concentrations, this will be a minor effect because then the probability is high that the hydrogen-bonded water wire already ends in a carboxylate oxygen before the wire acquires the spatial freedom to get looped on itself. We revisit this assumption in the discussions.

In each reaction complex, the proton is conducted from the acid to the base through a hydrogen-bonded water wire. The rate at which this conduction takes place depends strongly on the length of the wire and is governed by the solvent fluctuations. The rate constant of proton conduction $k[n, a]$ will depend on the number of water molecules separating the acid and the base. We use the following expression for this rate:

$$k[n, a] = ak_0\Delta^{n-2} \tag{3}$$

The rate constant $k[n, a]$ is thus assumed to decrease exponentially with the number of water molecules, which (assuming Arrhenius-like behavior) is equivalent to assuming that the free-energy barrier to the reaction increases linearly with water wire length $n-1$. The exponential decrease with increasing wire length can be understood from the fact that conduction of the proton from the acid to the base is only possible when all n hydrogen bonds in the connecting

chain of water molecules allow for the transfer. Hence, the rate constant is multiplied with a factor Δ for every additional element in the connecting chain of water molecules. The value of Δ is largely governed by the probability that the water molecule possesses the correct hydrogen-bond configuration to conduct the proton charge. As will be discussed later, the proton conductivity of the water molecule is likely determined by the strength of the second hydrogen bond to the oxygen atom of the water molecule. The decrease of the rate constant with increasing number of intervening water molecules is illustrated in Fig. 1b. In this figure $\Delta=0.2$, however, it is important to note that the model also includes the possibility that long-range proton transfer is absent as a reaction pathway, in which case $\Delta = 0$. The rate constant $k[n, a]$ scales with the number a of acetate oxygens because every acetate oxygen represents a parallel channel for taking up the proton. Due to the reaction each state will decay following:

$$S[n, a](t) = S[n, a](0)e^{-k[n,a]t}. \tag{4}$$

The survival probability of the acid can be determined by the sum over the population of reactive configurations:

$$R(t) = \sum_n \sum_a^{2^{n-1}} S[n, a](t), \tag{5}$$

This description is similar to the theory used to describe donor-acceptor electron transfer in solid solutions [30].

The time dependence of the states $S[n, a](t)$ is not only determined by the PT rate $k[n, a]$, but also by the diffusion of acetate between the shells. This diffusion will influence the proton-transfer dynamics. For instance, for large initial separations of HPTS and acetate, the acetate likely first hops to a closer shell before it actually takes up the proton. To include diffusion in the model, we transfer the diffusion coefficient of acetate to a characteristic time that acetate needs to hop over a distance of a single water molecule, using the Einstein-Smoluchowski relation ($\tau_D = l^2/6D$, with l the distance over which the molecule moves). Using this relation, we obtain a characteristic hopping rate $k_d = 1/\tau_D$. The acetate hopping

10

is described in the following manner. First, the occupation of the states $S[n, a]$ are translated into probability densities $p_a[n]$ that define the probability that an oxygen in shell n is an acetate oxygen:

$$p_a[n](t) = \frac{1}{P_w^{(2^{n-1}-1)} 2^{n-1}} \sum_a S[n, a](t) a \qquad (6)$$

Initially, all $p_a[n]$ will be equal to P_a. However, when the reaction proceeds, the probability $p_a[n]$ will decrease with decreasing value of n, because the lower shells get depleted by the distant-dependent proton-transfer reaction. Hence, after some time, $p_a[n]$ approaches P_a only for large n. The diffusion will thus lead to a net flow of acetates from higher to lower shells. To describe this flow, the hopping time τ_D should be subdivided into inward, outward, and within-shell hopping rates. To conserve the occupation of the shells in the absence of any reaction, the inward rate constant k_i has to be half the outward rate constant k_o, because the average number of acetates doubles with each additional shell number. In view of the number of possible positions in each shell, the within-shell hopping rate constant will be intermediate between k_i and k_o. We approximate this rate constant to be $\sqrt{2}k_i$. As a result, we obtain $k_i = k_d/(1 + \sqrt{2} + 2)$. The diffusion can best be described by dividing the transfer events in net flows between shells n and $n - 1$. The change of the number of acetate oxygens in shell n due to the net flow to shell $n - 1$ is:

$$\frac{dp_a[n](t) 2^{n-1}}{dt} = -(p_a[n](t) - p_a[n - 1](t)) k_i 2^{n-1} \qquad (7)$$

The change in the number of acetate oxygens contained in shell n results in changes $dS[n, a](t)/dt$ that are given by (using equation (6)):

$$\frac{1}{P_w^{(2^{n-1}-1)}} \sum_{a=1}^{2^{n-1}} \frac{dS[n, a](t) a}{dt} = -(p_a[n](t) - p_a[n - 1](t)) k_i 2^{n-1} \qquad (8)$$

Now we have to find the contribution of each state $S[n, a](t)$ to the total loss $(p_a[n](t) - p_a[n - 1](t)) k_i 2^{n-1}$ of the acetate oxygens out of shell n. We define $f_d[n, a](t)$ with the condition that $\sum_a f_d[n, a](t) a = 1$. The chance for donating an acetate to the inner shell will be proportional to the number of acetates. Hence, the change $f_d[n, a](t)$ should scale with a. We thus arrive at:

11

$$f_d[n, a](t) = \frac{aS[n, a](t)}{\sum_{a=1}^{2^{n-1}} a^2 S[n, a](t)}. \tag{9}$$

and, using equation (8):

$$\frac{dS[n, a](t)}{dt} = -f_d[n, a](t)(p_a[n](t) - p_a[n - 1](t))k_i 2^{n-1} P_w^{(2^{n-1}-1)} \tag{10}$$

The distribution over the states $S[n - 1, b](t)$ in the inner shell that receive the acetates will be different from the distribution over the states that donate acetates. We define $f_r[n - 1, b](t)$ with the condition that $\sum_b^{2^{n-2}} f_r[n - 1, b](t) = 1$. The chance to receive an acetate oxygen scales with the number of vacancies in the shell. When an acetate oxygen is received, the state $S[n - 1, b - 1](t)$ is transferred to the state $S[n - 1, b](t)$. A special case is the state $S[n - 1, 1](t)$ which is generated when an acetate is transferred from any of the 2^{n-1} states $S[n, a](t)$. We arrive at:

$$f_r[n - 1, b](t) = \frac{\{2^{n-2} - (b - 1)\}S[n - 1, b - 1](t) - \{2^{n-2} - b\}S[n - 1, b](t)}{\sum_{a=1}^{2^{n-1}} 2^{n-2} S[n, a](t)}, 2 \le b \le 2^{n-2}$$

$$\tag{11}$$

and

$$f_r[n - 1, 1](t) = \frac{\sum_{a=1}^{2^{n-1}} 2^{n-2} S[n, a](t) - \{2^{n-2} - 1\}S[n - 1, 1](t)}{\sum_{a=1}^{2^{n-1}} 2^{n-2} S[n, a](t)}. \tag{12}$$

For the change in the receiving state $S[n - 1, b](t)$ we use:

$$\frac{dS[n - 1, b](t)}{dt} = -f_r[n - 1, b](t) \sum_{a=1}^{2^{n-1}} \frac{dS[n, a](t)}{dt}, \tag{13}$$

which implies that the total number of states is conserved in the diffusion. In calculating the total effect of diffusion, the net flows for all combinations $n \rightarrow n - 1$ are added, which implies that all shells will gain population from shell $n + 1$ and will lose population to shell $n - 1$, except of course for shell $n = 1$ that only gains population from shell $n = 2$. The time dependencies of the states $S[n, a]$ are calculated by time integrating the coupled equations with a fourth-order Runge Kutta algorithm.

EXPERIMENTAL RESULTS

In Fig. 2, transient infrared spectra measured for a solution of 10 mM HPTS dissolved in D_2O are shown. The spectra represent the response in the frequency region corresponding to the aromatic ring vibrational modes of the photo-acid HPTS and its conjugated photo base PTS^{*-} at five different delay times. The spectrum measured at 1 ps after the excitation represents the direct change in the aromatic ring system induced by the electronic excitation. With increasing delay, the amplitude of the bands at 1480 and 1540 cm^{-1} decreases and a new vibrational band centered at 1503 cm^{-1} arises. This latter band is assigned to the PTS^{*-} conjugated photo base, and its rise marks the transfer of a deuteron from (deuterated) HPTS to the D_2O solvent. In addition to the spectral changes of the aromatic ring vibrational modes of HPTS, we observe a broadband infrared absorption directly after the excitation (Fig. 3). The amplitude of this absorption is linear in the pump intensity, which shows that this absorption is not the result of multi-photon excitation processes. The broadband infrared absorption extends up to frequencies of 2800 cm^{-1} for a solution of HPTS in H_2O. Above this frequency, the broadband infrared response is obscured by the strong absorption of the OH stretch vibrations of the H_2O solvent. For the solutions in D_2O we observe a similar broadband infrared absorption up to frequencies of 2200 cm^{-1}. Above this frequency the broadband absorption can no longer be observed because of the strong absorption of the OD stretch vibrations of D_2O.

In Fig. 4 the dynamics of the broadband absorption and the conjugated photo base PTS^{*-} are shown for a sample with an HPTS concentration of 10 mM. The broadband infrared absorption shows a partial decay with the same time constant as the rise of the conjugated photo base. The time constant of this partial decay/rise is 90 ps for a solution of HPTS in H_2O and 220 ps for a solution of HPTS in D_2O.

In Fig. 5 the dynamics of the the broadband continuum, acetic acid carbonyl stretch, and HPTS* and the conjugate photobase PTS^{*-} are shown for a solution of 10 mM HPTS and 1 M acetate in H_2O. These transients show the data at delays >1 ps. At earlier delay times the

signals also show a pulse-width limited component that results from the PT reaction between direct ground-state complexes of HPTS and acetate. This fast initial signal contribution was also found in earlier work on the proton transfer between HPTS and acetate [19,20]. It is seen that the broadband infrared continuum shows a complete decay that coincides with the decay of the aromatic ring vibrations of HPTS*. Also shown in Fig. 5 is the rise of the carbonyl stretch vibration of acetic acid that reflects the proton uptake by the acetate base. This rise follows that of the PTS*$^-$ band at 1503 cm^{-1}.

In Fig. 6 the decay of the broadband infrared continuum is shown for different acetate concentrations dissolved in H_2O (Fig. 6a) and D_2O (Fig. 6b). The data are plotted on a logarithmic scale which illustrates that the decays are highly non-exponential, particularly at short delay times. It is also seen in Fig. 6 that the rate of decay of the broadband infrared continuum strongly increases with increasing acetate concentration and that the deuteron transfer decay in D_2O is substantially slower than proton transfer in H_2O.

In Fig. 7a the early time dynamics of the spectral response of the carbonyl stretch vibration of acetic acid is shown. Within the first 10 ps after the excitation the absorption shifts to higher frequencies and becomes narrower. In Fig. 7b the first spectral moment of the absorption band of the carbonyl stretch vibration is shown as a function of delay. It is seen that this moment shifts to higher frequencies with a time constant of ∼4 ps. These changes in spectral response can be explained from the reorganization of the solvation shell of the carboxylate group following the uptake of the proton. Similar effects have been observed before for carbonyl vibrations of dye molecules [31]. We also studied the effects of additional ions on the rate of proton transfer. In Fig. 8 the broadband infrared absorption is shown as a function of delay for a solution containing 10 mM HPTS, 1 M of acetate, and different concentrations of NaBr. The addition of NaBr is observed to lead to a slowing down of the dynamics, especially for delays >30 ps. For this study we choose NaBr as the additive, because Na$^+$ and Br$^-$ ions do not quench the excited HPTS ions. For solutions containing Cl$^-$ or I$^-$ ions rather strong quenching effects were observed.

DISCUSSION

Interpretation

The excitation of HPTS directly leads to a broadband induced infrared absorption, as is illustrated in Fig. 3. The dynamics of this broadband absorption closely follow the dynamics of the vibrational modes of HPTS*, and are complementary to the rise of the carbonyl stretch mode of acetic acid in solutions containing acetate (Fig. 5). Hence, we assign the initial broadband response to the response of protons/deuterons that are loosely bound to HPTS* following photoexcitation. The broadband nature of the absorption of these proton/deuterons results from the strong hydrogen bonding between the weakened O-H group of the excited HPTS and the nearest water molecules. In earlier measurements of fluorescence intensities by Weller it was also found that the excitation of HPTS leads to a strengthening of the hydrogen bond. For strongly hydrogen-bonded O-H/O-D groups, the absorption band of the O-H/O-D stretch vibration is very broad because of the strong anharmonic coupling to the low-frequency hydrogen-bond modes [32–35]. The broadband infrared response is not completely structureless: a broad feature is observed at 2500 cm^{-1} (Fig. 3) that could due to the loosely bound proton being solvated by two additional water molecule in an Eigen-like structure [36].

In the absence of acetate, the broadband infrared response shows a partial decay with a time constant of 90/220 ps for solutions of HPTS in H_2O/D_2O (Fig. 4). These time constants have been observed previously in optical studies of HPTS dissociation in H_2O/D_2O. The partial decay shows the same dynamics as the complementary rise of the conjugated photobase PTS*$^-$ (Fig. 4). Hence, the partial decay of the broadband infrared absorption is assigned to the transfer of the proton/deuteron from HPTS to the solvent. The final resulting broadband infrared absorption thus reflects the absorption of fully hydrated protons/deuterons.

Fig. 5 shows that the release of the proton/deuteron by HPTS* leads to a complementary

rise of an aromatic ring vibrational response that is characteristic for the conjugate photo base PTS*−. This observation implies that the electronic structure of PTS*− significantly differs from that of HPTS*. This finding agrees with the results of a theoretical study in which it was found that the release of the proton is accompanied by a charge transfer from the oxygen atom to the aromatic ring system [15]. This charge transfer is an essential feature of the reaction as it turns PTS*− into a weak base. We thus conclude that the proton transfer induced by exciting HPTS involves two sequential electronic rearrangements. The first rearrangement is directly induced by the excitation of the HPTS molecule, and leads to a significant weakening of the covalent bond of the OH group. As a result, the proton becomes loosely bound, and gives rise to broadband infrared absorption. The second electronic rearrangement occurs when the proton leaves the HPTS* molecule, and involves the electron transfer of the oxygen atom to the aromatic ring system. This transfer leads to the vibrational, optical absorption, and fluorescence responses that are characteristic for the conjugate photo base PTS*−.

In Fig. 5 it is seen that the rise of the carbonyl stretch vibration of acetic acid shows exactly the same dynamics as the rise of the conjugated photo base PTS*−. The dynamics of these two signals are also exactly complimentary to the decays of the broadband infrared absorption of the loosely bound proton and the vibrational modes of the excited HPTS*. These observations imply that there is not a long-lived intermediate in the proton transfer reaction pathway from HPTS* to acetic acid. If there would have been such a long-living intermediate, the rise/decay of PTS*−/HPTS* would have shown faster dynamics than the rise of the carbonyl stretch vibration of acetic acid. Clearly, after leaving HPTS*, the proton does not wander around before arriving at the acetate base. It should be noted that this is different for other bases [23,37]. In a recent study of the proton-transfer reaction between HPTS and the much weaker base tri-chloro-acetate, the carbonyl stretch of tri-chloro-acetic acid was observed to show a much slower rise than the vibrational response of PTS*−, indicating that many protons are taken up for a longer time by the solvent before they react with the base [23]. This observation is not surprising, since tri-chloro-acetic-acid is a slightly

stronger acid than HPTS* ($pK_a(HPTS^*) \sim 1$, $pK_a(CCl_2CO_2H) = 0.52$). Apparently, when the base is sufficiently weak, PT to solvent followed by scavenging of the proton by the base becomes the dominant reaction channel.

Data Analysis with the Conduction Model

The solid curves shown in Fig. 6 are obtained by fitting the conduction model described in section III to the data. The parameters resulting from the fits are $k_0 = (1.2 \text{ ps})^{-1}/(1.8 \text{ ps})^{-1}$ for H_2O/D_2O and $\Delta = 0.2$ for both H_2O and D_2O. The diffusion is described by translating the diffusion constant of acetate to a characteristic time for hopping between solvation shells. Using the diffusion constant for acetate in water, a distance of 2.8 Å(the O-O distance in water), and the Einstein-Schmoluchowski relation, we obtain a characteristic rate for acetate hopping, $k_d = 1/\tau_D = (8.3 \text{ ps})^{-1}$. This rate is slower than PT in complexes with n=2-4 (equation (3)). The results in Fig. 6 show that the conduction model provides an excellent fit of the data at all delay times, including the highly non-exponential early time kinetics. The model fully accounts for the dependence of the proton transfer on base concentration: the acceleration of the proton transfer with increasing base concentration directly follows from the change in the statistical distribution of acetate with concentration. In Fig. 9a the distribution of the acetate density is shown at different delay times, obtained with the conduction model for a solution of 1 M acetate in H_2O using the best-fit model parameters given above. It is clearly seen that at early delays the lower shells are quickly depleted, because these shells show the highest proton-transfer reaction rate. In Fig. 9b, the distribution of reactive configurations corresponding to the density profiles in Fig. 9a is presented as a function of shell number at various delay times. With increasing delay, this distribution shifts to higher shells and becomes narrower, as a result of the depletion of the lower shells by the proton-transfer reactions.

The distribution of intermolecular separations over which proton/deuteron transfer occurs is illustrated in Fig. 10a,b, and is compared to the initial distribution of reactive com-

plexes. It is seen that most proton transfers occur in complexes in which HPTS and acetate are separated by 2-3 water molecules. This finding implies that the hydrogen-bonded water-wires that actually contribute to proton transfer are not long enough to become looped on themselves. Hence, the assumption that the proton transfer path branches as 2^n with each subsequent solvation shell is reasonable in this context. For complexes in which HPTS and acetate are separated by 4 or more water molecules, the fraction of proton transfers is significantly lower than the statistical fraction of acetates, which shows that for these larger separations many of the acetates diffuse first to a shell closer to the HPTS before they react. As a consequence, for complexes with only 1 or 2 water molecules separating the acid and the base, the fractions of proton transfer events are larger than the statistical fractions of acetate. However, for concentrations of 2 and 4 M of acetate the effect of diffusion is surprisingly small: the distribution of proton transfers is not very different from the statistical distribution. Clearly, diffusive transport of the reactants becomes more important as the base concentration decreases. In this low-concentration regime, the conduction model yields similar kinetics as the two-step Eigen-Weller framework. Nevertheless, the conduction model remains conceptually different since even at low base concentration there will still be a distribution of reaction distances instead of one well-defined reaction distance. However, the presence of this distribution no longer determines the reaction rate, since at low concentration the overall rate is completely determined by the diffusion of the reactants (i.e. the rate at which reactive complexes are formed, not the rate of PT within these complexes).

From the values of k_0 it follows that the proton/deuteron conduction shows an isotope effect of 1.5. This KIE is smaller than that for acid dissociation ($\sim$2.4) inline with expectations, since direct PT between HPTS* and acetate in aqueous solution has a much larger reaction asymmetry, ΔG = -21 kJ/mol, than PT between HPTS* and water, ΔG = +3 kJ/mol. The isotope effect of 1.5 is the same as has been found for the transfer of protons and deuterons in water/heavy water. It should also be noted that this isotope effect does not point to tunnelling as being the dominant mechanism of proton/deuteron transfer. Tunnelling processes are generally expected to lead to much higher isotope effects, because

tunnelling rates show an exponential dependence on the mass.

The value of $\Delta = 0.2$ means that the transfer rate decreases quite rapidly with increasing number of water molecules in the wire connecting HPTS and acetate. This decrease is partly compensated by the doubling of the number of possible positions for the acetate oxygen with each additional water molecule in this wire. Hence, the number of possible reaction paths strongly increases, while the rate per path decreases. The net effect is that the transfer takes place over an average wire length of 3 water molecules. The value of $\Delta = 0.2$ can be understood from the hydrogen-bond configuration that is required to enable proton conduction. Several theoretical studies have shown that proton conduction requires the hydrogen-bond structure to acquire a near-planar structure in which the hydrogen atoms of the water molecule each donate a hydrogen bond to the oxygen of neighboring water molecule and the oxygen atom accepts only one hydrogen bond. Thus, from a structural perspective, the factor Δ likely relates to the probability that a water molecule acquires a hydrogen-bond structure in which one of the hydrogen bonds to the oxygen atom is broken. Since the probability that one of the donated hydrogen bonds is broken is the same, a value of $\Delta = 0.2$ implies that the probability for a water molecule to be three-fold coordinated is approximately 40%. Assuming a statistical distribution of broken and intact hydrogen bonds, a percentage of 40% three-fold coordinated water molecules implies that each of the four hydrogen bonds of the water molecule has a probability of ~ 0.82 to be intact. This probability in turn means that the average number of hydrogen bonds equals $4 \times \sim 0.82 \sim 3.3$, which is in quite good agreement with the average number of hydrogen bonds per water molecule in room temperature liquid water. Proton conduction from the acid to the base requires all n intervening water molecules to acquire a three-fold coordination, making the transfer rate scale with Δ^n.

The results in Fig. 8 show that the proton transfer becomes slower when Na^+ and Br^- ions are added to the solution. The results in this figure show that the ions have very little effect on the proton transfer occurring at early delay times up to ~ 30 ps. For longer delay times, the presence of ions leads to a significant slowing down of the proton transfer.

These observations show that the effects of ions on the transfer increases with increasing separation of HPTS and acetate. It should be noted that the observed slowing down of the proton transfer cannot be explained from an increase in viscosity: the increase in viscosity upon adding NaBr is only a few percent, which is negligible in comparison to the observed effect on the proton transfer. The slowing down is also not the result of a slower direct transfer to the solvent. We find that the time constant of this transfer is slightly increased from 90 ps to 110 ps upon addition of 2 M NaBr. Similar effects were found in previous optical studies on the effects of added salts on the rate of proton transfer from HPTS to water [38,39]. However, this effect is negligible in comparison to the slowing down of the transfer of the proton from HPTS to acetate. The data can be very well described with the conduction model when we take $\Delta=0.2$ within the first three shells, and a lower value of Δ from the fourth shell onward. The value of k_0 remains the same at all concentrations. The results of the calculations are shown as the solid curves in Fig. 8 For the solution of 1 M NaBr, we find $\Delta = 0.15$ for $n > 3$, for the solution of 2 M NaBr we find $\Delta = 0.1$ for $n > 3$. The decrease in Δ follows from the effects of the Na^+ and Br^- ions on the hydrogen-bond structure. The ions restructure the water molecules to form hydration shells, which affects the probability of generating configurations that enable proton conduction from HPTS to acetate. Interestingly, the effect of the ions is very small in the first $\sim$30 ps, in which time interval the proton transfer is dominated by reactive complexes in which HPTS and acetate are separated by only 1-3 water molecules. Apparently, the ions have little effect on the water structure in the first few hydration layers of the hydroxyl group of the HPTS molecule.

Long-Range Adiabatic Proton Transfer

The results of the previous sections show that acid-base reactions in water do not take place at a single, well-defined reaction distance, as was assumed in the Eigen-Weller picture and in the SCK model that is based on this picture. Instead, there exists a range of distances

over which the proton can be transferred from the acid to the base. We also find that the reaction is essentially long range, involving proton transfers over an average number of 2-3 water molecules, depending on base concentration. Long-range character is a well-known phenomenon for electron transfer and energy transfer. For intermolecular proton transfer long-range character is less obvious. An argument against long-range proton transfer is that the proton is too heavy a particle to be harpooned from an acid to a distant base. Indeed, in non-protic solvents proton transfer is only possible in a reaction complex in which the acid and the base are connected by a single hydrogen bond. In protic solvents like water the situation is different, as the solvent molecules can form conduction wires that transfer the proton charge. This mechanism has been previously proposed to be active in excited state intramolecular proton transfer (ESIPT) reactions, based on the observation that some of these reactions can only take place in protic solvents [40–42]. For these systems it has been proposed that an O-H group of a solvent molecule forms a conduction bridge between the intramolecular proton donating and proton accepting groups. Long-range proton conduction has also been proposed to occur in biological systems, especially in trans-membrane proteins that conduct protons from one side of the membrane to the other side [43–46]. There has also been substantial theoretical work demonstrating that protons are transferred in liquid water via conduction through hydrogen-bonded water wires [27–29]. For instance, with Car-Parrinello molecular dynamics simulations it was found that the neutralization of H_3O^+ and OH^- in water involves proton conduction through several intervening water molecules [28]. The rate of this neutralization is largely determined by the solvent fluctuations that have to establish the right configuration for the proton conduction.

Based on our observations and recent theoretical work, we now arrive at the following picture for the mechanism by which a proton is released by an excited photo-acid dissolved in liquid water. Directly after the excitation, the proton is loosely bound showing short-lived delocalizations along hydrogen-bonds connected to the active site of the acid. The short-lived delocalizations closely follow the solvent dynamics, which lead to transient hydrogen-bond configurations of the nearby water molecules that favor the uptake of (part) of the proton

21

charge. At some moment the proton escapes, which means that from that time on the proton charge is shared by water molecules only. For HPTS in H_2O this will happen after a characteristic time of 90 ps, which, in view of the fast hydrogen-bond and orientational dynamics of liquid water, implies that the escape is a rare event. When the acetate base is added, the picture is nearly the same. The loosely bound proton again shows short-living delocalizations through the fluctuating hydrogen-bond network, but the delocalization length required to escape from HPTS can be shorter, depending on the distance to the base and the strength of the base. The base will trap the proton as soon as the delocalized proton reaches the base with sufficient amplitude. In view of the large mass of the proton, the relatively long distance over which the proton has to be transferred and the observed isotope effect it is highly unlikely that the proton reaches the base via a tunnelling process. Instead, the reaction involves adiabatic proton transfer within the hydrogen-bonded acid-base pair similar to that described by J. T. Hynes in his pioneering studies of acid ionization in water [1,2,10].

In the adiabatic proton-transfer picture, the barriers to PT are formed by i) water molecules not having the correct hydrogen-bond configuration to conduct the proton and ii) solvent polarization conditions strongly favoring the reactants. In the initial reactant state the proton is near the acid, with possible delocalization up to the barrier formed by the first water molecule that does not have the correct hydrogen-bonded configuration for taking up the proton charge. This initial situation is illustrated in the free-energy curve A in the top panel of Fig. 11. Due to solvent fluctuations, the barriers in the proton coordinate fall and rise continuously, until a symmetric proton potential develops and coincidentally all barriers are below the ground vibrational level of the proton (free energy curve B, top panel Fig. 11). In this solvent configuration, the proton wave function delocalizes up to the base. It should be noted that this is a rare event: the proton must wait near the acid until eventually a short-living favorable solvent configuration for transfer arises. Further solvent fluctuations stabilize this product state after which the proton has very little probability of escaping from the base (free energy curve C, top panel Fig. 11). Implicit in the description above is that

the direct PT between HPTS* and acetate proceeds via a *concerted*, long-range reaction pathway involving adiabatic proton transfer. We should note that in the original work of Ando and Hynes [2,10], the concerted (long-range) pathway was found to be disfavored in simple acid ionization. A two-step process, involving first ion-pair formation followed by the break-up of the ion-pair was found to be energetically more favorable. However, here the context is significantly different, with the product state free-energy surface considerably below (ΔG = -21 kJ/mol) either the reactant state or the ion-pair free-energy surfaces. This situation seems to favor the concerted pathway (Fig. 11, lower panel), since it does not require the production of a higher-energy intermediate (weak acid ion-pair formation). Ion-pair formation was found to be rate-limiting in the case of HF ionization in water [10], therefore, the opening of the concerted pathway is likely the reason for the large increase in PT rate when acetate is added to solution.

The rate constant for PT in a fully adiabatic picture obeys a simple Arrhenius-like expression [47]:

$$k = \frac{\omega_s}{2\pi} e^{-\Delta G^\ddagger / RT},$$ (14)

where ω_s is an appropriate solvent frequency. The activation energy $\Delta G^\ddagger$ contains terms representing the reorganization of the solvent, the asymmetry of the reaction, and the changes in zero-point vibrational energy of the hydrogen-bond and the proton/deuteron vibrations going from the reactant to the transition state. For current purposes we can write:

$$\Delta G^\ddagger = \Delta G^\ddagger_S + \Delta ZPE^\ddagger_{H/D},$$ (15)

where $\Delta ZPE^\ddagger_{H/D}$ represents the change in the zero-point vibrational energy of the proton/deuteron going from reactant to transition state, and $\Delta G^\ddagger_S$ is the complete solvent reorganization energy including contributions from the asymmetry of the reaction and changes in zero-point energy of the hydrogen-bond vibrations. The zero-point energy is higher for the proton than for the deuteron in the reactant state, and decreases going from the reactant to the transition state. Hence, $\Delta ZPE^\ddagger_H$ has a larger negative value than $\Delta ZPE^\ddagger_D$, which

23

makes the total activation energy $\Delta G^{\ddagger}$ lower for the proton than for the deuteron. The complete solvent reorganization energy, $\Delta G_S^{\ddagger}$, will be very similar for H_2O and D_2O. Hence, we can anticipate that the isotope effect of the reaction is determined primarily by differences of the solvent frequency and the zero-point energy of the proton/deuteron vibration.

By combining equations (14) and (15) with the distance dependent rate constant of equation (3), we obtain an expression that relates the conduction model parameters to those more commonly used in the adiabatic PT literature:

$$k_{0H/0D}\Delta^{n-2} = (\omega_{sH/sD}/2\pi)e^{-(\Delta ZPE_{H/D}^{\ddagger}+\Delta G_S^{\ddagger})/RT},\tag{16}$$

where k_{0H} and k_{0D} denote the values of k_0 for solutions in H_2O and D_2O, respectively. The isotope effect is thus given by

$$\frac{k_{0H}}{k_{0D}} = \frac{\omega_{sH}}{\omega_{sD}}e^{(\Delta ZPE_D^{\ddagger}-\Delta ZPE_H^{\ddagger})/RT},\tag{17}$$

We find the isotope effect of ~ 1.5 to be present in the parameter k_0, and not in the parameter Δ. Therefore, k_0 not only contains the solvent frequency, but also the zero-point energy $\Delta ZPE_{H/D}$ of the proton/deuteron vibration. The ratio of the solvent frequencies ω_{sH}/ω_{sD} can be estimated from the values of the Debye relaxation time constants in H_2O and D_2O, because these time constants represent the time scale on which the liquid can adapt to a change in (local) electric field. The Debye times are 8.3 and 10.4 ps for H_2O and D_2O, respectively [48]. Using these time constants we find for the ratio ω_{sH}/ω_{sD} a value of 1.25, which is still lower than the observed isotope effect of ~ 1.5. The remaining isotope effect is contained in the zero-point energy. If we substitute the ratios k_{0H}/k_{0D} and $\omega_{sH}\omega_{sD}$ in equation (17), we find $\Delta ZPE_D^{\ddagger} - \Delta ZPE_H^{\ddagger} = \sim 40$ cm^{-1}. If we assume that the zero-point energies scale with the square root of the mass, we thus find that $\Delta ZPE_H^{\ddagger} = \sim$-130 cm^{-1} and $\Delta ZPE_D^{\ddagger} = \sim$-90 cm^{-1}. These changes represent the changes in zero-point energy of the proton/deuteron going from the reactant state to the transition state. These energies are small compared to the zero-point energies of the vibrations of strong O–H and O–D chemical bonds. It can thus be concluded that the O–H/O–D bond is very much weakened in the

excited state of HPTS and/or that the transition state of the reaction is not very different from the reactant state. This is generally the case for asymmetric, strongly downhill reactions [47], which indeed applies to the reaction of HPTS* and acetate. We can also estimate the value of $\Delta G_S^\ddagger$ from our findings:

$$\Delta G_S^\ddagger(n) = -(n-2)RT\ln\Delta, (n>2) \tag{18}$$

This equation gives the solvent contribution to the activation energy as a function of the number of water molecules separating the acid and the base. Using $\Delta = 0.2$ (and T $= 300$ K) we thus find that $\Delta G^\ddagger(n) \sim (n-2)\times335$ cm^{-1} ($\sim (n-2)\times4$ kJ/mol). This increase in activation energy with water wire length can be understood in terms of the distance between reactant and product free energy surfaces in the solvent coordinate. This is illustrated in the lower panel of Fig. 11, where the $n=2$ and $n=4$ free energy surfaces of the product state (dotted parabolas) are shown to be displaced from the $n=3$ surface.

In the discussion above we have considered the adiabatic PT case, which appears to be most appropriate for the current system. It would, however, not to be difficult to extend the description to the case of non-adiabatic PT in which the proton has to tunnel to go from the reactant to the product state. In that limit the reaction rate can be described by a similar Arrhenius equation as equation (14) where the activation energy contains terms representing the solvent reorganization and the asymmetry of the reaction and a term representing the difference in vibrational energy between the reactant and the product [49]. An important difference with the expression for the rate of adiabatic PT is that the pre-factor contains the tunneling probability of the proton. The tunneling probability is strongly isotope dependent and shows an exponential dependence on the distance the proton has to tunnel [49]. This means that in the case of non-adiabatic PT, the isotope effect will be stronger than in the case of adiabatic PT. In the situation of long-range non-adiabatic PT in solvent-separated acid-base complexes, it could be that the distance the proton has to tunnel increases with the number of separating water molecules. This distance dependence can be accounted for in the conduction model by including an additional (exponential) distance dependence in

the parameter k_0.

It should be noted that despite the earlier discussion, it is not completely clear which hydrogen-bond configurations the water molecules have to acquire to enable proton conduction. It has been proposed that the water molecules have to adopt a near-planar three-fold hydrogen-bonded configuration to enable proton transfer. However, it could be that the requirements on this structure are not that severe. For instance, ice is a quite good proton conductor and for ice most of the water molecules will be tetrahedrally coordinated by four hydrogen bonds. We hope that the present findings will stimulate further theoretical work on the hydrogen-bond configurations of water that allow for intermolecular proton transfer and the role of the exothermal character of the reaction in promoting concerted reaction pathways over step-wise mechanisms.

CONCLUSIONS

We studied the mechanism of intermolecular aqueous proton transfer between the photo-acid 8-hydroxy-1,3,6-pyrenetrisulfonic acid (HPTS) and acetate by probing the vibrational responses of the photo-acid, the accepting base and the hydrated proton with femtosecond vibrational spectroscopy. The proton transfer from HPTS to acetate shows strongly non-exponential dynamics and an isotope effect of 1.5. Together with the observation of a loosely bound proton coincident with photoexcitation the results suggest that the proton transfer involves the conduction of protons through hydrogen-bonded water wires of different lengths connecting the acid and the base.

Based on this concept, we developed a conduction model that provides an excellent description of the data at all delay times and base concentrations. This model contains two parameters: a rate constant k_0 representing the characteristic rate of conduction of the proton over a single hydrogen bond, and the parameter Δ that defines the decrease of the reaction rate with each additional intervening water molecule. The base concentration dependence of the proton transfer follows from the change of the statistical distribution of

distances between HPTS and acetate. The values of k_0 are $(1.2/1.8 \text{ ps})^{-1}$ for the reaction in H_2O/D_2O. The value of Δ is 0.2, which likely corresponds to the probability that one of the hydrogen bonds to the oxygen atom of a water molecule is broken, thus yielding a three-fold hydrogen-bonded configuration that conducts the proton. The value of k_0 is strongly governed by the dynamics of the solvent, while Δ represents a structural parameter.

The conduction model also includes the effect of diffusion. For acetate concentrations ≥ 1 M diffusion does not play a significant role as most proton transfers occur in reaction complexes with 0-5 intervening water molecules that were already present before HPTS was excited. Only for reaction complexes with larger separations is translational diffusion of the reactants necessary to facilitate PT. Thus, the PT reaction is seen to evolve from solvent-fluctuation controlled PT within an effectively static acetate distribution at short delay times to diffusion-controlled PT at large delay times.

The addition of ions to the solution leads to a slowing down of the proton transfer, because the ions disturb the hydrogen-bond network of liquid water. However, the ions only affect the rate of proton transfer for reaction complexes that contain 4 or more intervening water molecules.

ACKNOWLEDGMENT

REFERENCES

[1] Staib, A.; Borgis, D.; & Hynes, J. T. *J. Chem. Phys.* **1995**, *102*, 2487.

[2] Ando, K.; & Hynes, J. T. *J. Phys. Chem. B* **1997**, *101*, 10464.

[3] Eigen M.; Kruse W.; Maass G.; & de Maeyer L. *Progress in Reaction Kinetics Vol. 2* (Pergamon Press, New York),**1964**, p. 285.

[4] Eigen, M. *Angew. Chem. Intern. Ed.* **1964**, *3*, 1-19.

[5] Weller, A. *Z. Electrochem.* **1954**, *58*, 849.

[6] Weller, A. *Z. Phys. Chem. Leipzig* **1958**, *17*, 224.

[7] Smoluchowski, M. von *Z. Phys. Chem.* **1917**, *92*, 129.

[8] Collins, F. C.; & Kimball, G. E. *J. Colloid Sci.* **1949**, *4*, 425.

[9] Rice, S. A. *Diffusion-limited Reactions* (Elsevier, Amsterdam) **1985**.

[10] Ando, K.; & Hynes, J. T. *J. Phys. Chem. A* **1999**, *103*, 10398.

[11] Pines, E.; Huppert, D.; & Agmon, N. *J. Chem. Phys.* **1988**, *88*, 5620-5630.

[12] Agmon, N.; Pines, E.; & Huppert, D. *J. Chem. Phys.* **1988**, *88*, 5631-5638.

[13] Solntsev, K. M.; Huppert, D.; Agmon, N.; & Tolbert, L. M. *J. Phys. Chem. A* **2000**, *104*, 4658.

[14] Tran-Thi, T.-H.; Gustavsson, T.; Prayer, C.; Pommeret, S.; & Hynes, J. T. *Chem. Phys. Lett.* **2000**, *329*, 421-430.

[15] Hynes, J. T.; Tran-Thi, T.-H.; & Granucci, G. *J. Photochem. Photobiol. A* **2002**, *154*, 3-11.

[16] Leiderman, P.; Genosar, L.; & Huppert, D. *J. Phys. Chem. A* **2005** *109*, 5965-5977.

[17] Pines, E.; Magnes, B.-Z.; Land, M. J.; & Fleming, G. R. *Chem. Phys. Lett.* **1997**, *281*,

413-420.

[18] Genosar, L. T.; Cohen, B.; & Huppert, D. *J. Phys. Chem. A* **2000**, *104*, 6689-6698.

[19] Rini, M.; Magnes, B.-Z.; Pines, E.; & Nibbering, E. T. J. *Science* **2003**, *301*, 349-352.

[20] Rini, M; Pines, D.; Magnes, B.-Z.; Pines, E.; & Nibbering, E. T. J. *J. Chem. Phys.* **2004**, *121*, 9593-9610.

[21] Mohammed, O. F.; Pines D.; Dreyer J.; Pines E; & Nibbering E. T. J. *Science* **2005**, *310*, 83-86.

[22] Mohammed, O. F.; Pines D.; Dreyer J.; Pines E; & Nibbering E. T. J. *ChemPhysChem* **2005**, *6*, 1625.

[23] Mohammed, O. F.; Pines D.; Nibbering E. T. J.; & Pines E. *Angew. Chem. Intern. Ed.* **2007**, *46*, 1458.

[24] Kiefer, P. M.; & Hynes, J. T. *J. Phys. Chem. A* **2003**, *107*, 9022. and refs. therein.

[25] Weller, A. in *Progress in Reaction Kinetics Vol. 1, G. Porter Ed.* (Pergamon Press, New York), **1961**, p. 189.

[26] Siwick, B. J.; & Bakker, H. J. *J. Am. Chem. Soc.* **2007**, to be published.

[27] Marx, D.; Tuckerman, M. E.; Hutter, J; & Parrinello, M. *Nature* **1999**, *397*, 601-604.

[28] Geissler, P. L.; Dellago, C.; Chandler, D.; Hutter, J.; & Parrinello M. *Science* **2001**, *291*, 2121.

[29] Lapid, H.; Agmon, N; Petersen, M. K.; & Voth, G. A. *J. Chem. Phys.* **2005**. *122*, 1.

[30] Lin, Y.; Dorfman, R. C.; & Fayer, M. D. *J. Chem. Phys.* **1989**, *90*, 159.

[31] Chudoba, C.; Nibbering, E. T. J.; & Elsaesser T. *Phys. Rev. Lett.* **1998**, *81*, 3010.

[32] Witkowski, A. *J. Chem. Phys.* **1967**, *47*, 3645.

[33] Marechal, Y.; & Witkowski, A. *J. Chem. Phys.* **1967**, *48*, 3637.

[34] Bratos, S. *J. Chem. Phys.* **1975**, *63*, 3499.

[35] Boulil, B.; Henri-Rousseau, O.; & Blaise, P. *Chem. Phys.* **1988**, *126*, 263.

[36] Headrick, J. M.; Diken, E. G.; Walters, R. S.; Hammer, N. I.; Christie, R. A.; Cui, J.; Myshakin, E. M.; Duncan, M. A.; Johnson, M. A.; & Jordan, K. D. *Science* **2005**, *308*, 1765.

[37] Hynes, J.T. *Nature* **2007**, *446*, 270.

[38] Huppert, D.; Kolodney, E.; Gutman, M.; Nachliel, E. *J. Am. Chem. Soc.* **1982**, *104*, 6949.

[39] Leiderman, P.; Gepshtein, R.; Uritski, A., Genosar, L.; & Huppert, D. *J. Phys. Chem. A* **2006**, *110*, 13686.

[40] Chapman, C. F.; & Maroncelli, M. *J. Phys. Chem.* **1992**, *96*, 8430.

[41] Lee, S.-I.; & Jang, D.-J. *J. Phys. Chem.* **1995**, *99*, 7537.

[42] Marks, D.; Zhang, H.; Borowicz, P.; Waluk, J.; Glasbeek, M. *J. Phys. Chem. A* **2000**, *104*, 7167.

[43] Akeson, M.; & Deamer, D. W. *Bioph. J.* **1991**, *60*, 101.

[44] Brewer, M. L.; Schmitt, U. W.; & Voth, G. A. *Bioph. J.* **2001**, *80*, 1691.

[45] Pomes, R.; & Roux, B. *Bioph. J.* **2002**, *82*, 2304.

[46] Yan, S.-H.; Zhang, L.; Cukier, R. I.; & Bu, Y.-X. *ChemPhysChem* **2007**, *8*, 944.

[47] Kiefer, P.M.; & Hynes, J.T. *J. Phys. Chem. A* **2003**, *107*, 9022.

[48] Kaatze, U. *Chem. Phys. Lett.* **1993**, *203*, 1.

[49] Borgis, D.; & Hynes, J. T. *J. Phys. Chem.* **1996**, *100*, 1118.
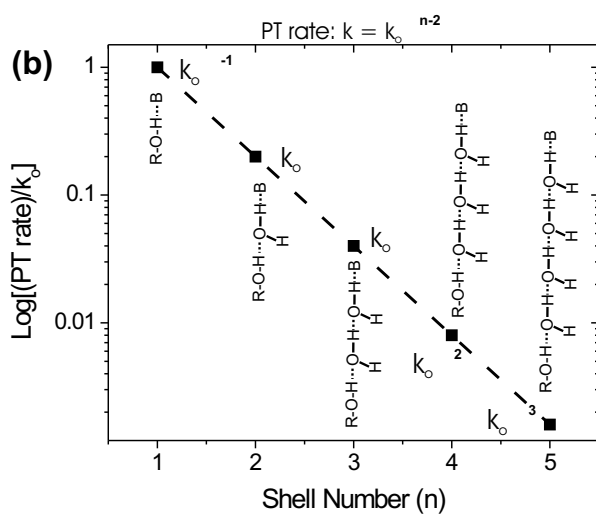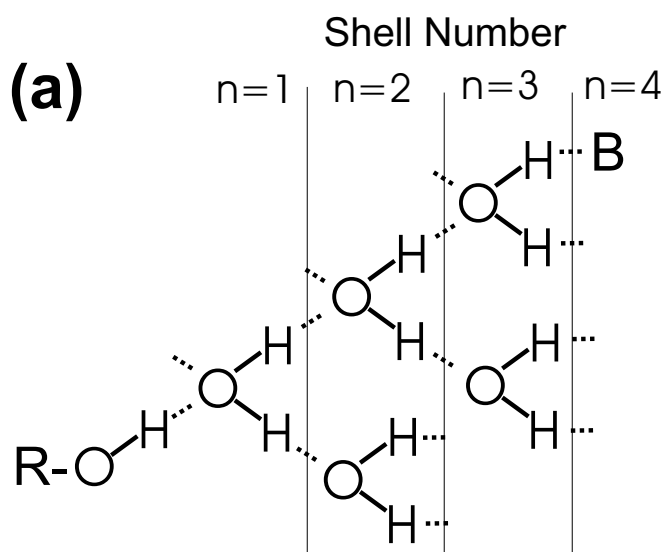
FIG. 1. Schematic pictures illustrating the conduction model. (a) the model hydrogen bond network for water connecting the OH group of the HPTS molecule with the base. (b) the dependence of the PT on the length of the water wire connecting the acid and the base decreases exponentially with the shell number.
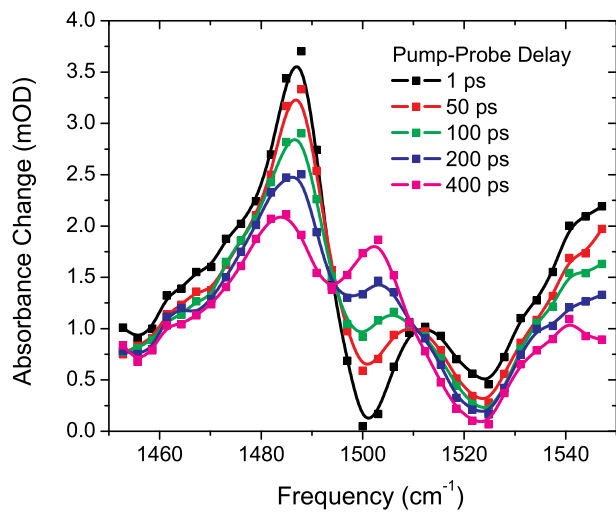
FIG. 2. Transient spectra of the vibrational bands of HPTS* and its conjugated photo base PTS*$^-$ near 1500 cm^{-1} at five different delays after excitation of a 10 mM HPTS solution in D$_2$O.
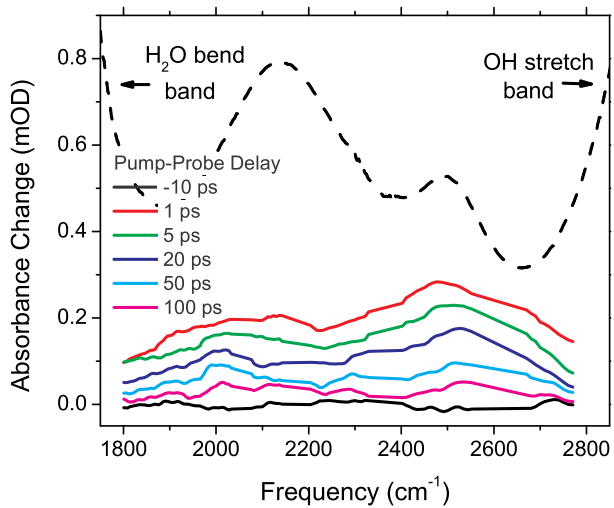
FIG. 3. Transient spectra showing the broadband infrared absorption at five different delays after excitation for a 10 mM HPTS solution in H_2O containing 1 M acetate. For comparison, the linear absorption spectrum of the solution is also shown. The sample is relatively transparent in the region between the strong H_2O bend and OH stretch bands of the solvent.
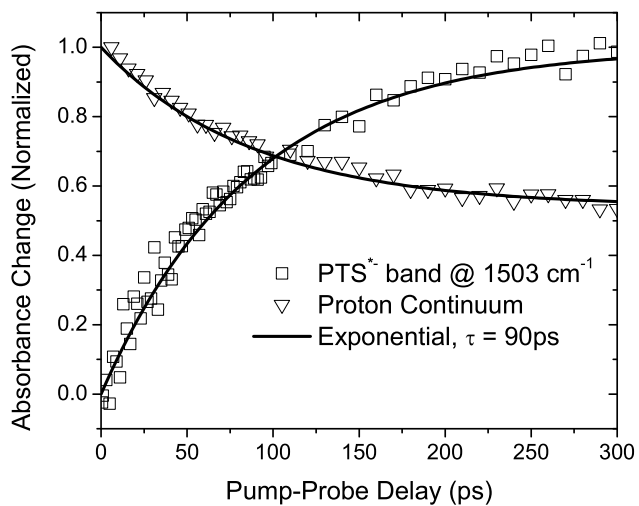
FIG. 4. Broadband infrared absorption at 1900 cm^{-1} as a function of delay for a solution of 10 mM of HPTS. Also shown is the rise of the signal of the conjugated photo base PTS*$^{-}$ measured at 1503 cm^{-1}.
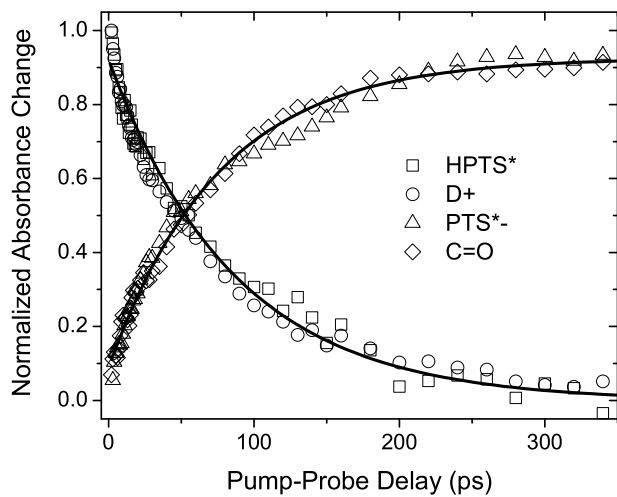
FIG. 5. Responses of HPTS* at 1430 cm^{-1}, the loosely bound deuteron at 1900 cm^{-1}, PTS*$^-$ at 1503 cm^{-1}, and the acetic acid carbonyl stretch at 1720 cm^{-1}, as a function of delay for a solution of 10 mM HPTS and 1 M acetate in D$_2$O.
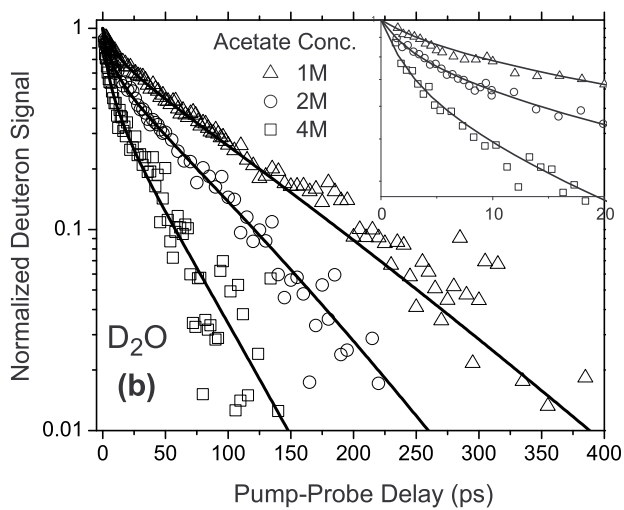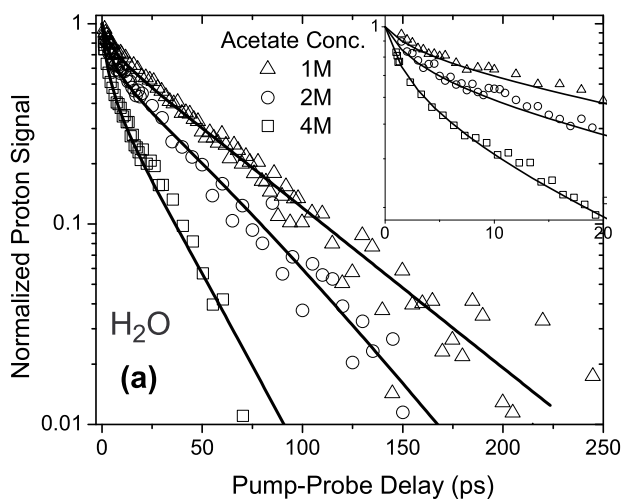
FIG. 6. Response of the broadband infrared continuum as a function of delay for solutions of 10 mM of HPTS and 1, 2, and 4 M of acetate in H_2O (a) and D_2O (b). In the inset the response measured in the first 20 ps is shown, illustrating the highly non-exponential character of the proton transfer. The solid lines are calculated curves using the conduction model described in the text.
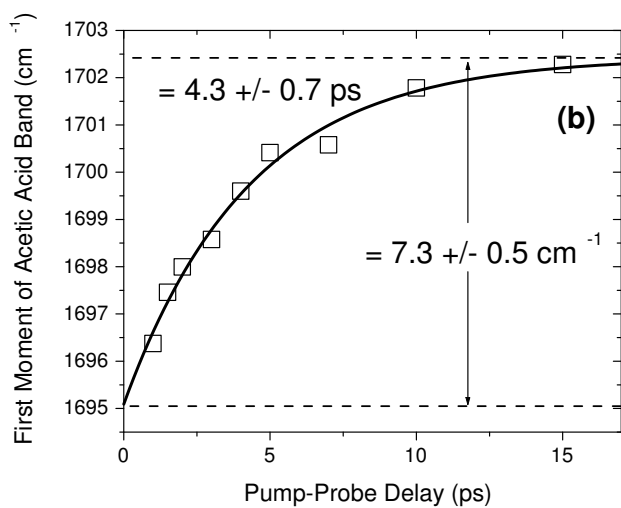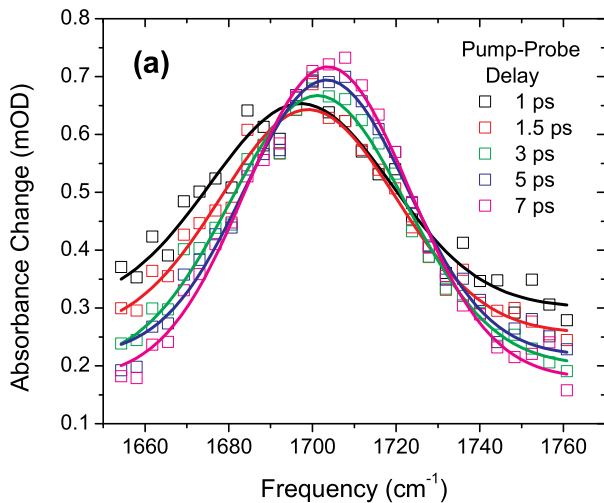
FIG. 7. Spectrum (a) and first spectral moment (b) for the carbonyl stretch of acetic acid as a function of delay measured for a solution of 10 mM HPTS and 2 M of acetate in D_2O. The band shifts to higher frequencies with 7.3 cm^{-1} on a timescale of 4.3 ps. These dynamics correspond to hydrogen bond rearrangements following the uptake of the proton by acetate.
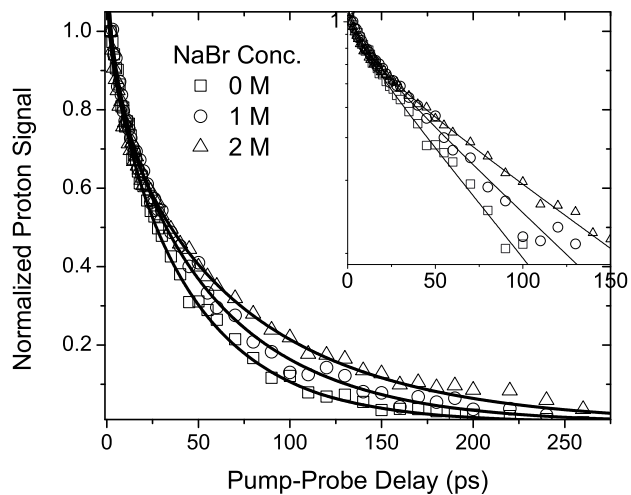
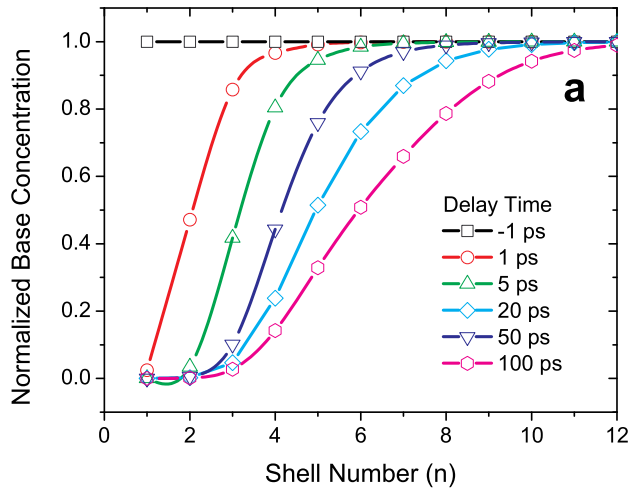FIG. 8. Response of the loosely bound proton measured at 2500 cm^{-1} as a function of delay for solutions containing 10 mM of HPTS, 1 M of acetate, and different concentrations of NaBr in H$_2$O. In the inset, the response is shown on a logarithmic scale.
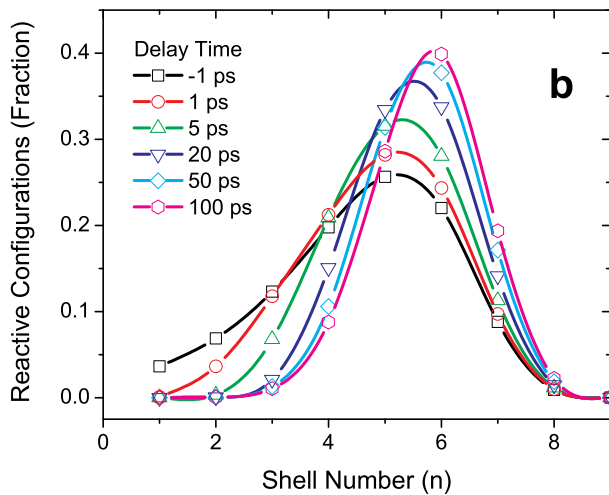
FIG. 9. Figure a: distribution of the density of acetate as a function of shell number at six different delay times, determined for a solution of 10 mM HPTS and 1 M acetate in H_2O. Figure b: the distribution of reactive complexes (see Fig. 1b) that corresponds to the concentration/density profiles shown in (a).
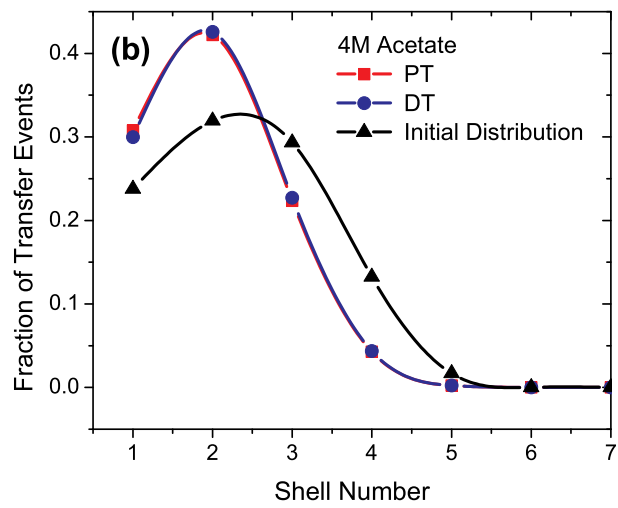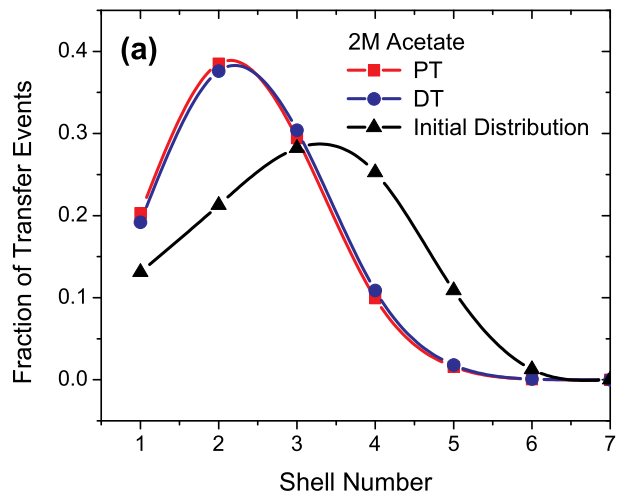
FIG. 10. Fraction of proton/deuteron transfer events in initially solvent separated complexes (i.e. excluding the direct contact pairs) as a function of the number of the number of water molecules separating HPTS and acetate, determined for solutions of 10 mM HPTS and 2 M acetate (Figure a) or 4 M acetate (Figure b). For comparison, the initial statistical distributions of acetate at these concentrations are shown.
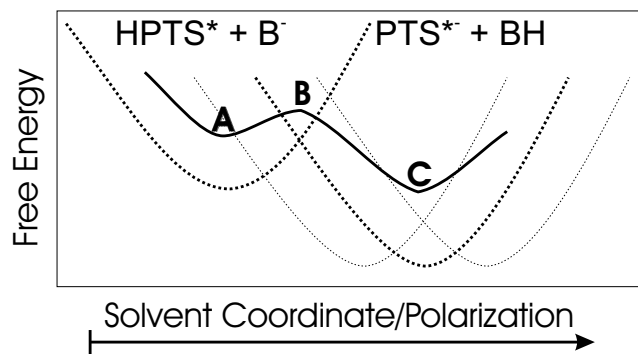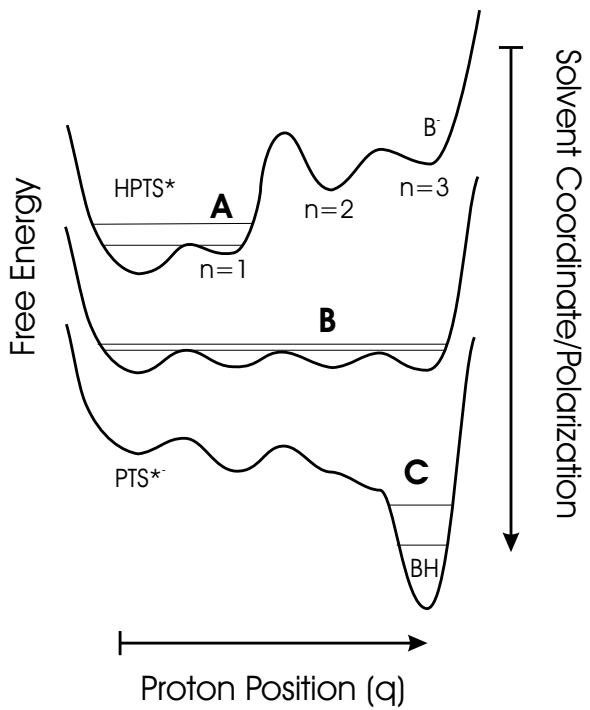
Free Energy

Solvent Coordinate/Polarization

HPTS*
A
n=1
n=2
n=3
B⁻
B
PTS*⁻
C
BH

Proton Position (q)

Free Energy

HPTS* + B⁻   PTS*⁻ + BH

A
B
C

Solvent Coordinate/Polarization

FIG. 11. Schematic picture illustrating long-range adiabatic PT between HPTS* and acetate in aqueous solution. The top panel shows the effect of solvent fluctuations on the proton potential. The first two vibrational energy levels for the proton are shown as horizontal dashed lines. Free energy surface A represents the reactant state proton potential, B the transition state and C the product state. The bottom panel shows the solvent (diabatic) free energy surfaces in the reactant and product states (bold dotted parabolas) and the lowest proton vibrational level at various solvent coordinates (bold solid line). The solvent coordinates corresponding to the surfaces shown in the top panel are also labeled A-C. The two dotted product state solvent parabolas represent the effect of changing the length of the water-wire. Lengthening the water-wire is equivalent to shifting the product state parabola to the right, which increases the free-energy barrier of the reaction.